On the Influence of Porosity on the Portevin-Le Chatelier Effect in Sintered Iron

E.S. Palma

Sintered irons of four different porosities were strained in tension at temperatures between 295 (room temperature) and 873 K. Serrated stress-strain curves and high work hardening in the temperature range from 333 to 693 K, for all porosities, were characteristic of dynamic strain aging. The activation energy for the onset of serration was ±0.82 eV and was independent of porosity. On the contrary, the parameter β from the relation for dislocation density increased with increasing porosity.

Keywords
effects of porosity, effects of temperature, mechanical properties, sintered iron

1. Introduction

THE PORTEVIN-LE CHATELIER effect (PLC) is a manifestation of dynamic strain aging (DSA). Specimens tested in certain ranges of temperature and strain rate show serrated stress-strain curves as a result of interaction between mobile dislocations and diffusing solute atoms. In this phenomenon, solute atoms are attracted by and move to dislocations, forming solute atmospheres around them (Ref 1-4). An increase in the resistance to dislocation movement, because of pinning of dislocations by solute atoms and the strengthening of the dislocations forest (Ref 2, 5-8), results in variations in the mechanical properties of materials and usually causes an increase in strength and a decrease in ductility (Ref 2, 9-11).

Recently, much work has been done in order to understand the phenomenon involving DSA and PLC in metals from both experimental and theoretical viewpoints (Ref 12-14), while other studies have been concerned with the mathematical modeling of DSA (Ref 15-16).

Sintered materials, as distinguished from pore-free materials, have porosity as a distinguishing feature. The effects of pores on the mechanical properties of sintered materials have been intensively investigated and well documented (Ref 17-26). It is generally found that an increase in porosity leads to a decrease in yield stress, ultimate tensile stress (UTS), ductility, Young's modulus of elasticity, and so on. This effect has been associated with the dependence of the load-bearing cross section on porosity and, mainly, on the internal notch effect of pores. It is very well known that the notch effect is higher the smaller and more irregular the pores.

Although much literature exists about the effect of strain aging on the yield strength and flow strength of pore-free materials, and the effect of porosity on the mechanical properties of sintered materials, relatively little attention has been given to the influence of temperature and porosity on the PLC effect in sintered materials. The present work concentrates on the effect of porosity on the temperature dependence of the mechanical properties of sintered iron under tension. This work also discusses the influence of porosity on the initiation of the PLC effect in sintered iron.

E.S. Palma, Depto. de Engenharia Mecânica-UFMG, Av. Antônio Carlos, 6627 CEP.:31270.901, Belo Horizonte, MG, Brazil.

2. Experimental Procedures

2.1 *Materials*

A Höganäs ASC 100.29 iron powder was chosen for the present study. Its chemical composition is listed in Table 1, and Table 2 gives the particle size distribution.

The compaction pressure used to prepare tensile specimens, as shown in Fig. 1, was varied to give four different as-sintered porosities: 3.7, 6.2, 8.8, and 12.5. Sinterization of specimens was carried out for 30 min at 1150 °C in an atmosphere of cracked ammonia.

Microstructure analysis and phase identification were performed by light microscopy. A typical optical micrograph for porosity P_0 = 12.2% is shown in Fig. 2.

Table 1 Chemical composition of iron (wt %)

C	P	Cu	Si	Al	Mn	Cr	Ni	Fe
0.02	<0.01	0.02	0.10	0.05	0.03	<0.01	0.02	Bal

Table 2 Particle size distribution of iron powder

Particle size, μm	Content, wt %
230	0.3
200	0.9
152	9.8
44	28
<44	Bal

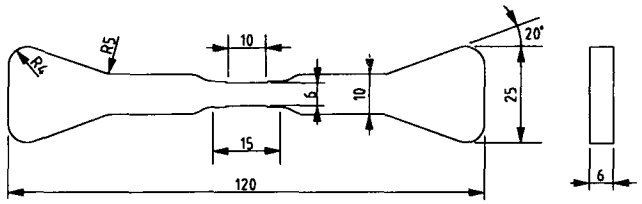

Fig. 1 Geometry of tensile specimen (dimensions in mm)

2.2 *Tensile Testing*

Tensile tests were carried out in a Zwick model 1498 universal testing machine, equipped with a furnace that controlled the temperature from 295 to 873 K. A Ni-Cr-Ni thermocouple with accuracy of ±2 °C was attached to the middle of the specimen for temperature measurements and control. Tests were performed at constant cross-head speeds of 0.18 mm/min, corresponding to an initial strain rate of $2.0 \times 10^{-4}\ s^{-1}$. Three or four specimens were tested under each temperature condition, and the average values of the properties (yield stress, UTS, ductility, Young's modulus of elasticity, etc.) were calculated. Longitudinal strains corresponding to each respective stress were measured and automatically recorded.

3. Results

3.1 *Effect of Porosity and Temperature on Mechanical Properties*

Figure 3 shows true tensile stress-strain curves at different temperatures for iron with $P_0 = 12.5\%$. In this figure, the characteristic serrated curves can be observed for temperatures between 363 and 573 K.

Figure 4 shows the 0.2% offset yield stress of iron as a function of temperature for three different porosities. The 0.2% offset yield stress decreases with increasing porosity and temperature. However, a plateau in the curves (or a small peak in the curve with $P_0 = 3.7\%$) occurs for $363 \le T \le 573$ K, within the DSA range.

The porosity and temperature dependence of UTS for iron are shown in Fig. 5. The behavior observed is as follows: At the beginning or at lower temperatures, the UTS decreases with increasing temperature and reaches a minimum around 350 K. The UTS then increases with increasing temperature and reaches a maximum around 500 K before decreasing with further increase in temperature. It also can be seen that the UTS increases with decreasing porosity content. At high temperatures, however, the influence of porosity on UTS becomes negligible.

The influence of porosity and temperature on the uniform strain of iron is shown in Fig. 6. Initially, the uniform strain decreases with increasing temperature and reaches a minimum around 400 K before increasing with further increase in temperature, until it reaches a maximum at about 700 K. The uniform strain then decreases with further increase in temperature. Similarly to the UTS, the uniform strain increases with decreasing porosity.

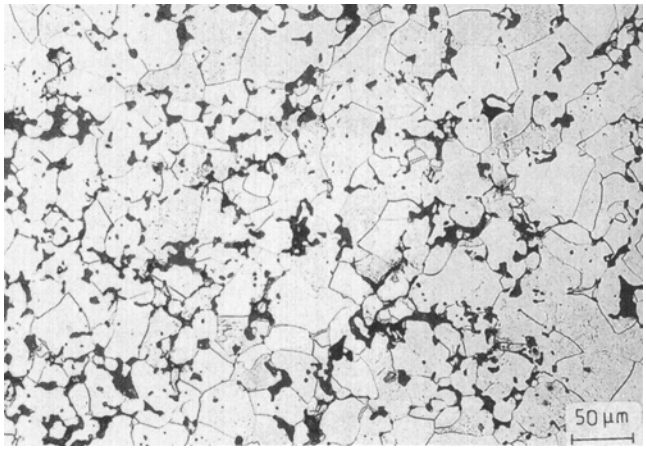

Fig. 2 Micrograph of iron with porosity $P_0 = 12.2\%$

3.2 *Activation Energy for Onset of Jerky Flow (Serrations)*

The model of DSA used in this study has been developed in detail in Ref 1, 5, and 17. In this model the density of mobile dislocations, ρ_{gl}, is assumed to increase as a power β of strain, i.e., $\rho_{gl} \sim \varepsilon^{\beta}$. Thus, the activation energy for the onset of serrations is calculated using the equation

$$\ln(\dot{\varepsilon}) = \ln(C) + \beta \ln(\varepsilon_c) - \frac{\Delta H_w}{kT} \qquad \text{(Eq 1)}$$

with

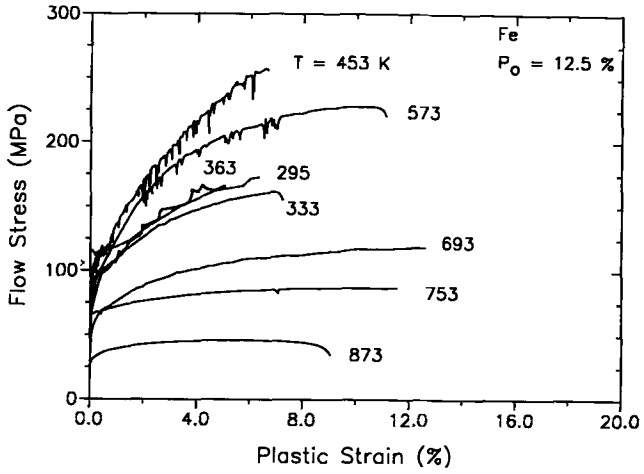

Fig. 3 Influence of temperature (from 295 to 873 K) on true stress-strain curves of iron with $P_0 = 12.5\%$

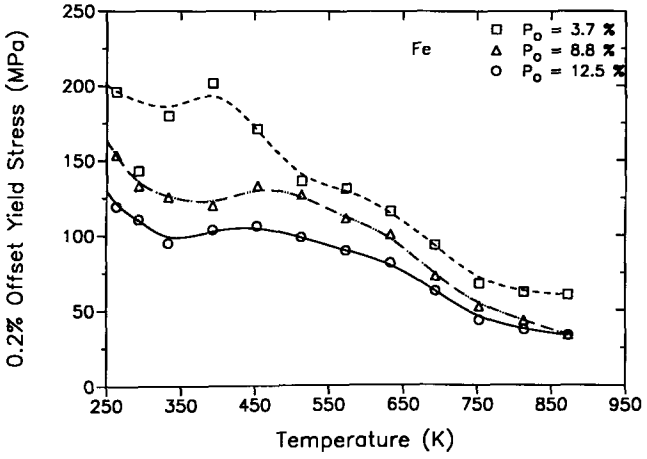

Fig. 4 Influence of temperature from (295 to 873 K) on 0.2% offset yield stress for irons with several porosity contents

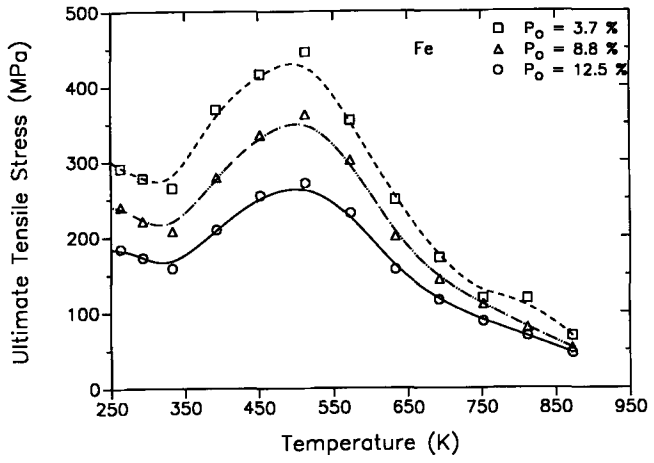

Fig. 5 Influence of temperature (from 295 to 873 K) on ultimate tensile strength for irons with several porosity contents

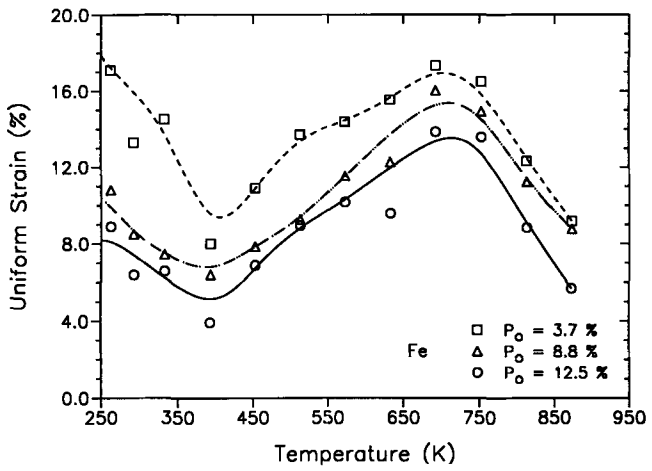

Fig. 6 Influence of temperature from (295 to 873 K) on uniform strain for irons with several porosity contents

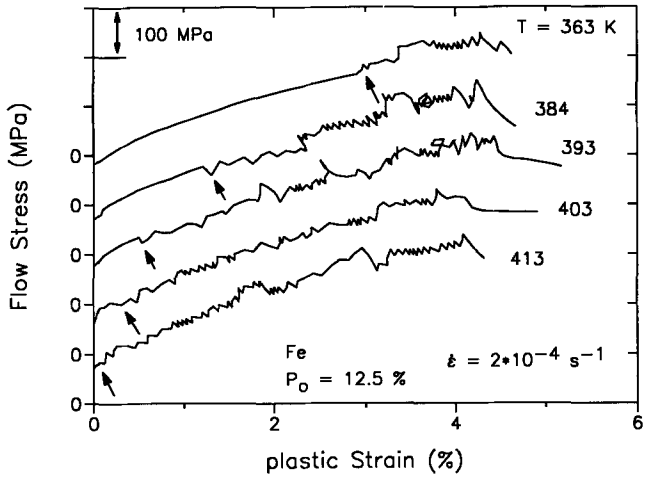

Fig. 7 Influence of temperature on the critical strain for the onset of serration, ε_c, for iron with P_0 = 12.5% ($\dot{\varepsilon} = 2 \times 10^{-4}\ s^{-1}$)

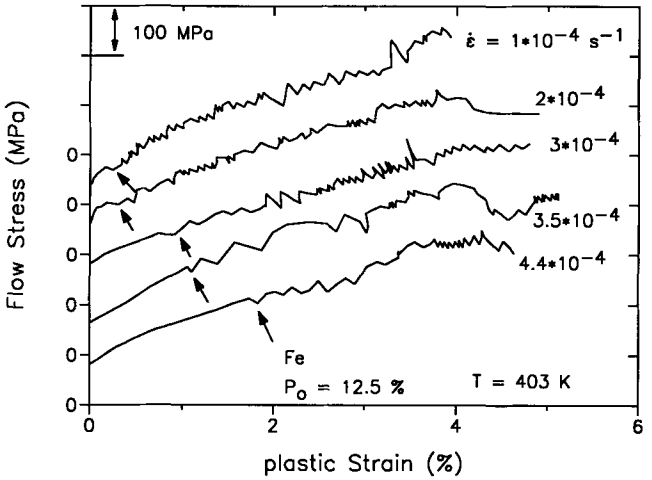

Fig. 8 Influence of strain rate on the critical strain for the onset of serration, ε_c, for iron with P_0 = 12.5% (T = 403 K)

Table 3 Activation energies for onset of dynamic strain aging and values of β for irons with different porosity contents, calculated using Eq 3 and 4

DSA parameter	Porosity P_0, % 3.7	6.2	8.8	12.5
$\Delta H_w/\beta$, eV	1.13	1.06	0.94	0.89
β	0.73	0.75	0.89	0.91
ΔH_w, eV	0.82	0.80	0.83	0.81

$$C = \frac{4kTD_0}{U_B M_T} \qquad \text{(Eq 2)}$$

where $\dot{\varepsilon}$ is the strain rate, ε_c is the critical strain rate for the onset of serrations, ΔH_w is the activation energy for the onset of serrations, k is Boltzmann's constant, T is absolute temperature, D_0 is a constant, U_B is the bond energy of atom, and M_T is Taylor's factor.

Therefore, by plotting $\ln(\dot{\varepsilon})$ against $\ln(\varepsilon_c)$ at the same temperature, one can obtain the value of β from the slope

$$\frac{\partial \ln(\dot{\varepsilon})}{\partial \ln(\varepsilon_c)} = \beta \qquad \text{(Eq 3)}$$

where T is constant. Similarly, the plot of $\ln(\varepsilon_c)$ against $1/kT$ at the same strain rate gives $(\Delta H_w + kT)/\beta$ as the slope

$$\frac{\partial \ln(\varepsilon_c)}{\partial(1/kT)} = \frac{\Delta H_w + kT}{\beta} \qquad \text{(Eq 4)}$$

where $\dot{\varepsilon}$ is constant. The activation energy for the onset of serrations, ΔH_w, can then be determined by this method, neglecting the factor kT, which is ~0.05 eV.

Using this approach, the critical strain for the onset of serration ε_c can be determined by plotting the stress-strain curve at

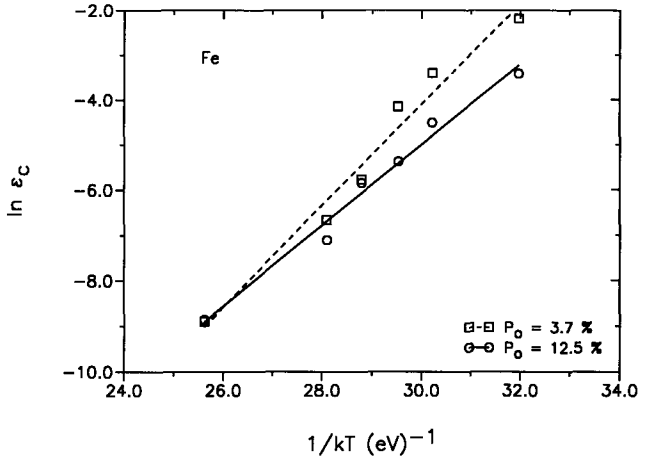

Fig. 9 Influence of temperature on the critical strain for the onset of serration, ε_c, for iron with P_0 = 12.5 and 3.7%

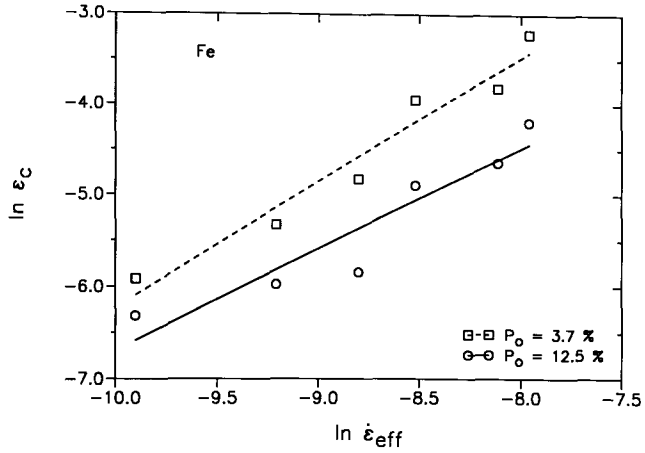

Fig. 10 Influence of actual strain rate on the critical strain for the onset of serration, ε_c, for iron with P_0 = 12.5 and 3.7%

different temperatures but at the same strain rate, and by plotting stress-strain curves at different strain rates but at the same temperature. These curves are shown in Fig. 7 and 8, respectively, for iron with 12.5% porosity. In these figures, the first critical strains for the onset of serration are identified by arrows. In both cases, smaller values of critical strain for the onset of serration, ε_c, can be observed by increasing the deformation temperature (where $\dot{\varepsilon}$ is constant) or by decreasing the strain rate (where T is constant).

Figures 9 and 10 show ε_c as a function of temperature and as a function of actual strain rate, respectively, for iron with P_0 = 12.5 and 3.7%. The values of $\Delta H_w/\beta$ and β were determined by using Eq 3 and 4 and the slope of Fig. 9 and 10. ΔH_w was calculated as the product of the two values, summarized in Table 3.

Figure 11 shows the plots of activation energies for onset of dynamic strain aging and the β exponent for iron as functions of porosity content. ΔH_w appears to be independent of porosity content, but the β values, on the other hand, increase with increasing porosity content.

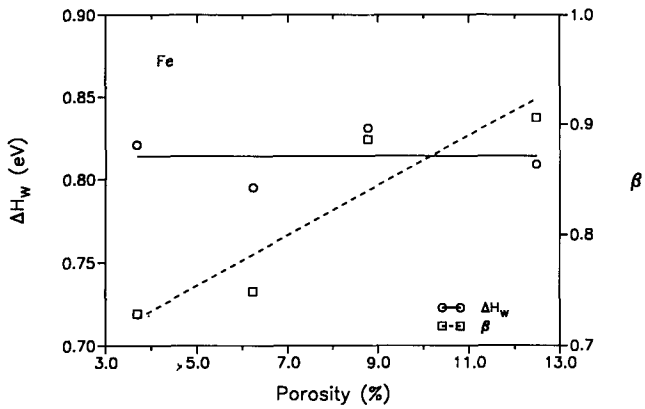

Fig. 11 Influence of porosity on the beginning of dynamic strain aging and β exponent values for iron

4. Discussion

The experimental results show that temperature influences the mechanical properties of sintered iron in the same way as for similar pore-free material. For example, at temperatures between 333 and 693 K, characteristic serrated curves that are due to the DSA effect (i.e., the repeated pinning of moving dislocations by solute atoms) have been frequently observed. Because this is a diffusion-controlled process, it reaches a maximum when the diffusion velocity of solute atoms becomes equal to the velocity of mobile dislocations, which is dependent on strain rate.

The results of the current study of critical strain for the onset of serration shows that the exponent β increases with increasing porosity. The values obtained for β are in good agreement with values in the literature, which lie between 0.5 and 1.0 (Ref 8, 11, 27). In order to explain the dependence of β on porosity, it must be observed that the values of β were determined from a macroscopically measured plastic strain, which was influenced by porosity. DSA, or jerky flow, is related to the dynamic interaction between diffusing solute atoms and mobile dislocations (i.e., the process takes place in a ferrite matrix). In a sintered porous material, inhomogeneous deformation takes place at localized small regions in the vicinity of pores. Increasing porosity leads to a higher concentration of plastic strain in these small regions. In order to maintain ε as a constant, the dislocation density is then increased. This is possible only if β values are increased.

Similarly, inhomogeneous plastic strain leads to an increase of $\Delta H_w/\beta$ values by decreasing porosity. The activation energy to begin DSA is obtained from the product of β and $\Delta H_w/\beta$, and, as expected, they are independent of porosity. The average value of ΔH_w for iron was 0.82 eV, and it was in good agreement with the values obtained from the literature (Ref 5, 28) for pore-free Armco iron. These values correspond to an activation energy for carbon diffusion in α-iron. Thus, the DSA is caused by diffusion of interstitial carbon solute atoms.

5. Conclusions

In summary, the following conclusions may be drawn from the experimental results, and from the publications discussed

above, about the influence of porosity on the temperature dependence of the deformation behavior of sintered iron:

1. The influence of temperature on the deformation behavior and mechanical properties of sintered iron is similar to its effect on pore-free iron.
2. At temperatures between 333 and 693 K, characteristic serrated curves were observed, which are due to DSA caused by the interaction between mobile dislocations and diffusing carbon solute atoms.
3. The exponent β in the dislocation density equations increases with increasing porosity due to pores, which lead to inhomogeneous plastic strain in sintered iron. Plastic strain takes place in the vicinity of pores. The β values in this work are in good agreement with those from the literature.
4. The values of activation energies for onset of DSA are independent of porosity. They are also in very good agreement with those determined for pore-free Armco iron and correspond to activation energy for carbon diffusion in α-iron.

Acknowledgments

The author is indebted to Alexandre Bracarense, Ph.D. for critical reading of the manuscript. The work described above was carried out in the Institut of Materials I, University of Karlsruhe, Germany, during the author's Ph.D. program.

References

1. P.G. McCormick, Model for the Portevin-Le Chatelier Effect in Substitutional Alloys, *Acta Metall.*, Vol 20 (No. 3), 1972, p 351-354
2. Y. Estrin, L.P. Kubin, and E.C. Aifantis, Introductory Remarks to the Viewpoint Set on Propagative Plastic Instabilities, *Scripta Metall. Mater.*, Vol 29 (No. 9), 1993, p 1147-1150
3. A.H. Cottrell, A Note on the Portevin-Le Chatelier Effect, *Philos. Mag.*, Vol 74 (No. 355), 1953, p 829-832
4. A. van den Breukel, On the Mechanism of Serrated Yielding and Dynamic Strain Aging, *Acta Metall.*, Vol 20 (No. 3), 1972, p 351-354
5. K. Hüttenbräucker, Das Zügige Verformungsverhalten Normalisierter Untereutektoider Kohlenstoffstähle, Ph.D. thesis, Karlsruhe University, 1977
6. R. Siegel, Temperatur- und Geschwindigskeitabhängigkeit der Reckalterung von Stahl, *Neue Hütte*, Vol 11, 1966, p 155-159
7. H. Conrad and S. Frederick, The Effect of Temperature and Strain Rate on the Flow Stress of Iron, *Acta Metall.*, Vol 10, 1962, p 1013-1020
8. F.J. Zerilli and R.W. Armstrong, The Effect of Dislocation Drag on the Stress-Strain Behavior of F.C.C. Metals, *Acta Metall.*, Vol 40 (No. 8), 1992, p 1803-1808
9. H.J. Harun and P.G. McCormick, Effect of Precipitation Hardening on Strain Rate Sensitivity and Yield Behaviour in an Al-Mg-Si Alloy, *Acta Metall.*, Vol 27, 1979, p 155-159
10. C.C. Li and W.C. Leslie, Effect of Strain Aging on the Subsequent Mechanical Properties of Carbon Steels, *Metall. Trans. A*, Vol 9A (No. 12), 1978, p 1765-1775
11. J.D. Baird and A. Jamieson, High Temperature Tensile Properties of Some Synthesized Iron Containing Mo and Cr, *J. Iron Steel Inst.*, Nov 1972, p 841-846
12. Y. Brechet and Y. Estrin, On the Influence of Precipitation on the Portevin-Le Chatelier Effect, *Acta Metall. Mater.*, Vol 43 (No. 3), 1995, p 955-963
13. S. Lou and D.O. Northwood, Effect of Strain Aging on the Strength Coefficient and Strain-Hardening Exponent of Construction-Grade Steels, *JMEPEG*, Vol 3 (No. 3), 1994, p 344-349
14. T. Shun, C.M. Wan, and J.G. Byrne, A Study of Work Hardening in Austenitic Fe-Mn-C and Fe-Mn-Al-C Alloys, *Acta Metall. Mater.*, Vol 40 (No. 12), 1992, p 3407-3412
15. L.P. Kubin and Y.Y. Estrin, Evolution of Dislocation Densities and the Critical Conditions for the Portevin-Le Chatelier Effect, *Acta Metall. Mater.*, Vol 38 (No. 5), 1990, p 697-708
16. P.G. McCormick and P.C. Ling, Numerical Modelling of the Portevin-Le Chatelier Effect, *Acta Metall. Mater.*, Vol 43 (No. 5), 1995, p 1969-1977
17. E.S. Palma, Verformunsgverhalten von Sintereisenwerkstoffen bei Einachsig Homogenen und Inhomogenen Beanspruchungen, Ph.D. thesis, Karlsruhe University, 1994
18. S. Klumpp, Quasistatisches und Zyklisches Verformungsverhalten Reiner und Legierter Sintereisenwerkstoffe, Ph.D. thesis, Karlsruhe University, 1992
19. M.S. Koval'chenko, Mechanical Properties of Sintered Materials, *Sov. Powder Metall. Mat.*, Vol 3, 1991, p 257-261
20. S.A. Firstov et al., Effect of Porosity on the Fracture Stress of Powder Materials in the Ductile Fracture Mechanism, *Sov. Powder Metall. Mat.*, Vol 5, 1992, p 451-455
21. M. Hammiuddin, Correlation between Mechanical Properties and Porosity of Sintered Iron and Steel—A Review, *Powder Metall. Int.*, Vol 18, 1986, p 73-76
22. H. Danninger, G. Jangg, B. Weiss, and R. Stickler, Microstructure and Mechanical Properties of Sintered Iron, *Powder Metall. Int.*, Vol 25, 1993, part I: p 111-117, part II: p 170-173
23. M. Nakamura and K. Tsuya, Strength and Elongation of Sintered Iron, *Powder Metall.*, No. 3, 1979, p 101-108
24. A. Fleck and A. Smith, Effect of Density on Tensile Strength, Fracture Toughness, and Fatigue Crack Propagation Behaviour of Sintered Steel, *Powder Metall.*, No. 3, 1981, p 121-125
25. A. Salak, V. Miskovic, E. Drudová, and E. Rudnayová, The Dependence of Mechanical Properties of Sintered Iron Compacts upon Porosity, *Powder Metallurgy Int.*, No. 6, 1974, p 128-132
26. G. Straffelini, V. Fontanari, and A. Molinari, Influence of Microstructure on Impact Behaviour of Sintered Ferrous Materials, *Powder Metallurgy*, Vol 38 (No. 1), 1995, p 45-51
27. L.P. Kubin and Y. Estrin, Evolution of Dislocation Densities and the Critical Conditions for the Portevin-Le Chatelier Effect, *Acta Metall. Mater.*, Vol 38 (No. 5), 1990, p 687-708
28. E. Macherauch, *Praktikum in Werkstoffkunde*, Braunschweig/Wiesbaden, 1989, p 138-144